Hypoxia-induced Bmi1 promotes renal tubular epithelial cell–mesenchymal transition and renal fibrosis via PI3K/Akt signal

Rui Du[a,b,*], Lin Xia[c,*], Xiaoxuan Ning[d,*], Limin Liu[b,*], Wenjuan Sun[b], Chen Huang[b], Hanmin Wang[b], and Shiren Sun[b]

[a]Department of Integrative Oncology and Radiation Oncology, Navy General Hospital, Beijing, 10037 China; [b]Department of Nephrology, [c]State Key Laboratory of Cancer Biology and Department of Digestive Diseases, and [d]Department of Geriatrics, Xijing Hospital, Fourth Military Medical University, Xi'an 710032, China

ABSTRACT **Hypoxia is an important microenvironmental factor in the development of renal fibrosis; however, the underlying mechanisms are not well elucidated. Here we show that hypoxia induces Bmi1 mRNA and protein expression in human tubular epithelial cells. We further demonstrate that Bmi1 expression might be directly regulated by hypoxia-inducible factor-1a (HIF-1a) under low oxygen. Moreover, chromatin immunoprecipitation and reporter gene assay studies reveal cooperative transactivation of Bmi1 by HIF-1α and Twist. Enforced Bmi1 expression induces epithelial–mesenchymal transition (EMT), whereas silencing endogenous Bmi-1 expression reverses hypoxia-induced EMT. Up-regulation of Bmi1 leads to stabilization of Snail via modulation of PI3K/Akt signaling, whereas ablation of PI3K/Akt signaling partially rescues the phenotype of Bmi1-overexpressing cells, indicating that PI3K/Akt signaling might be a major mediator of Bmi1-induced EMT. In a rat model of obstructive nephropathy, Bmi1 expression increases in a time-dependent manner. Furthermore, we demonstrate that increased levels of Bmi1, correlated with HIF-1α and Twist, are associated with patients with chronic kidney disease. We provide in vitro and in vivo evidence that activation of HIF-1a/Twist-Bmi1 signaling in renal epithelial cells is associated with the development of chronic renal disease and may promote fibrogenesis via modulation of PI3K/Akt/Snail signaling by facilitating EMT.**

Monitoring Editor
Jonathan Chernoff
Fox Chase Cancer Center

Received: Jan 27, 2014
Revised: May 19, 2014
Accepted: Jul 1, 2014

This article was published online ahead of print in MBoC in Press (http://www.molbiolcell.org/cgi/doi/10.1091/mbc.E14-01-0044) on July 9, 2014.

*These authors contributed equally to this work.

The authors declare no competing interests.

Address correspondence to: Shiren Sun (sunshiren@medmail.com.cn).

Abbreviations used: Bmi1, B lymphoma Mo-MLV insertion region 1 homologue; ChIP, chromatin immunoprecipitation; CKD, chronic kidney disease; DN, diabetic nephropathy; EMT, epithelial–mesenchymal transition; HBS, HIF-1α–binding site; HIF-1a, hypoxia-inducible factor-1a; HRE, HIF-1a responsive elementl; IgAN, immunoglobulin A nephropathy; PBS, phosphate-buffered saline; PI3K, phosphoinositide 3-kinase; PcG, Polycomb group; qRT-PCT, quantitative reverse transcription-PCR; siRNA, small interfering RNA; UUO, unilateral ureteral obstruction; ZO-1, zonula occludens-1.

INTRODUCTION

The epithelial–mesenchymal transition (EMT) is a developmental process in which epithelial cells lose their polarity and acquire the migratory properties of mesenchymal cells. EMT is a mechanism for generating primitive mesenchymal cells during gastrulation or mobile tumor cells or cells with properties of stem cells during cancer metastasis (Mani *et al*., 2008; Thiery *et al*., 2009). EMT has also been viewed as a principal source of fibroblasts in tissue fibrosis (Kalluri and Neilson, 2003). A recent breakthrough in renal fibrosis research revealed that induction of EMT also generates fibroblast-specific protein-1–positive fibroblasts (Iwano *et al*., 2002).This finding provides a crucial link between the acquisition of migration traits and collagen synthesis capability in epithelial cells undergoing EMT. Although the phenotypic association between EMT and fibrogenesis is firmly established, the underlying molecular mechanisms remain largely unknown.

The Polycomb group (PcG) genes encode a family of evolutionarily conserved regulators that were discovered in *Drosophila* as repressors of homeotic gene expression (Pirrotta, 1998). B lymphoma Mo-MLV insertion region 1 homologue (Bmi1), a member of the PcG family of transcription repressors, was originally identified as a Myc-cooperating oncogene in murine B- and T-cell lymphomas (van Lohuizen *et al.*, 1991; Bessede *et al.*, 2013). In humans, Bmi1 plays an essential role in maintaining the self-renewal of normal and malignant human mammary stem cells (Liu *et al.*, 2006). In addition, Bmi1 is also dysregulated in various human malignant neoplasms (Valk-Lingbeek *et al.*, 2004; Widschwendter *et al.*, 2007). Recently Bmi1 was demonstrated to induce epithelial–mesenchymal transition in human nasopharyngeal epithelial cells by repressing the tumor suppressor PTEN and downstream signal (Song *et al.*, 2009). Furthermore, Yang *et al.* (2010) reported that Bmi1 is essential in Twist-induced epithelial–mesenchymal transition in head and neck cancer cells. These results showed that Bmi1 might be a new regulator of EMT. Considering the importance of Twist in hypoxia-induced EMT in tubular epithelial cells and its relationship with Bmi1, we hypothesize that Bmi1 is involved in hypoxia-induced tubular epithelial cell EMT and renal fibrosis.

In this study, we characterize the effect of Bmi1 on hypoxia-induced EMT in tubular epithelial cells and renal fibrosis and investigate the underlying mechanisms. Our study provides the first evidence that hypoxia, via direct activation of Bmi1, promotes the renal tubular EMT phenotype and that Bmi1 expression might be induced by hypoxia-inducible factor-1a (HIF-1a) through the HIF-1a responsive element (HRE) located in the Bmi1-proximal promoter. Moreover, in vitro and in vivo studies reveal cooperative transactivation of Bmi1 by HIF-1α and Twist. We further show that Bmi1 is functionally involved in promoting tubular EMT after chronic injury, and the action of Bmi1 likely operates through stabilization of Snail via modulation of phosphoinositide 3-kinase (PI3K)/Akt signaling.

RESULTS

Hypoxia induces Bmi1 expression in tubular epithelial cells

Quantitative reverse transcription-PCR (qRT-PCR) analysis demonstrated that hypoxia significantly induced Bmi1 mRNA expression in human proximal tubular epithelial (HK-2) cells. As shown in Figure 1A,

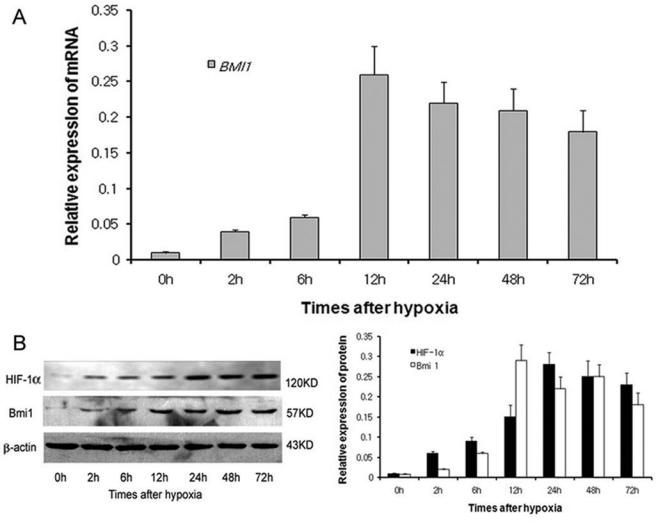

FIGURE 1: Hypoxia-induced Bmi1 mRNA and protein expression in HK-2. (A) qRT-PCR analysis of Bmi1 mRNA expression after 2, 6, 12, 24, 48, and 72 h of hypoxia. (B) Western blot analysis of HIF-1α and Bmi1 protein expression after different times of hypoxia.

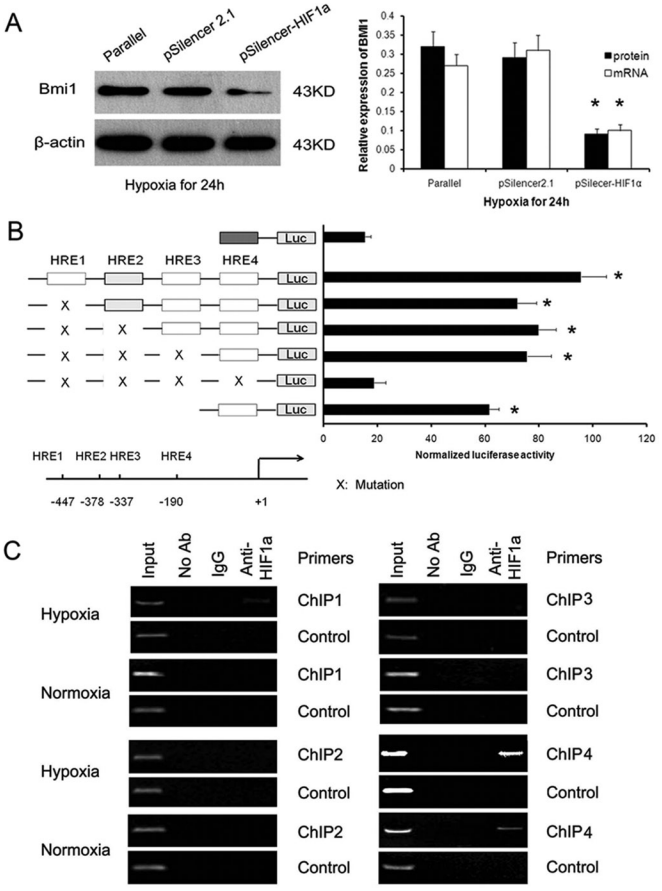

FIGURE 2: Bmi1 expression is directly regulated by HIF-1α. (A) qRT-PCR and Western blot analysis of Bmi1 mRNA and protein in siR-HIF-1α– and control vector–transfected HK-2 cells under low oxygen. (B) Relative luciferase activity of the Bmi1 promoter reporter gene. HK-2 cells were transfected with 20 ng of reporter constructs and 1 mg of pcDNA3.1-HIF-1a in combination with 0.2 ng of pRL-TK vector for 24 h. The luciferase results are reported as relative light units of firefly luciferase activity normalized with respect to the *Renilla* luciferase activity. Mean values from three independent experiments. *$p < 0.01$ compared with control. (C) Chromatin immunoprecipitation was performed to examine HIF-1a binding to the Bmi1 promoter in HK-2 cells under normoxia and low oxygen. Reaction controls include immunoprecipitations performed by using a nonspecific IgG monoclonal antibody (Cont IP), and PCR was performed by using whole-cell genomic DNA (Input). Representative example of three independent experiments.

the steady-state level of Bmi1 mRNA increased at 2 h, reached a peak at 12 h, and was sustained at least to 72 h after hypoxia treatment. Bmi1 protein was also induced after hypoxia in tubular epithelial cells, as demonstrated by Western blot analyses. As shown in Figure 1B, Bmi1 protein began to increase at 6 h after hypoxia, reached a peak at 24 h, and was sustained to at least 72 h, consistent with increase in hypoxia-inducible factor 1α (Figure 1A).

Bmi1 expression and transcriptional activation are directly induced by HIF-1a

To explore whether hypoxia-induced Bmi1 is mediated by HIF-1a, we transiently transfected HK-2 cells with a small interfering RNA (siRNA) plasmid containing an HIF-1a–targeting sequence. Repression of endogenous HIF-1a by siRNA in HK-2 cells under hypoxic conditions showed that the mRNA and protein levels of Bmi1 decreased (Figure 2A), showing that HIF-1a might regulate Bmi1 expression at the transcriptional level.

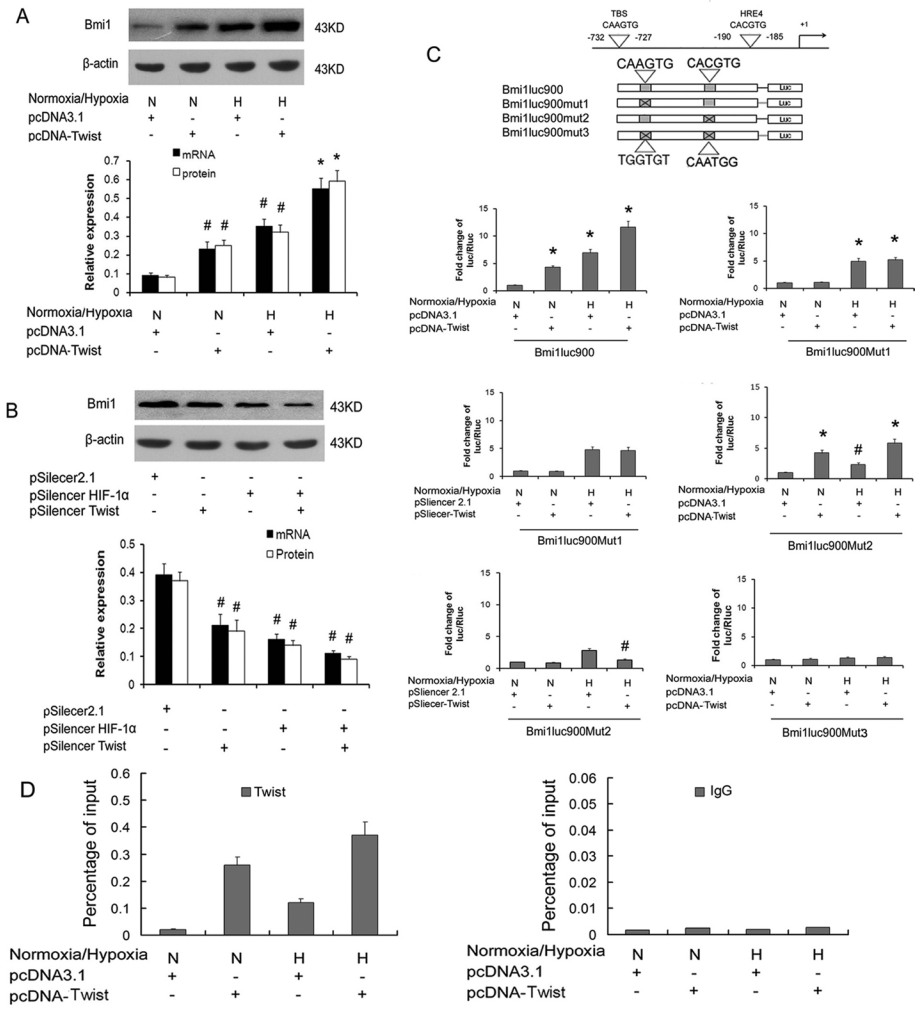

FIGURE 3: Cooperative activation of Bmi1 by HIF-1α and Twist. (A) qRT-PCR and Western blot analysis of Bmi1 mRNA and protein in Twist- or control vector–transfected HK-2 cells under normoxia or low oxygen. (B) qRT-PCR and Western blot analysis of Bmi1 mRNA and protein in siRNA against HIF-1α– and/or Twist- or control vector–transfected HK-2 cells under low oxygen. (C) Relative luciferase activity of the Bmi1 promoter reporter gene. The luciferase reporter constructs were made with the wild-type Bmi1 regulatory region (Bmi1-Luc900) and a Bmi1 regulatory region with the indicated base substitutions in the Twist-binding site (Bmi1-Luc900Mut1), the HBS (Bmi1-Luc900Mut1), or both in the E-box and HBS (Bmi1-Luc900Mut3). HK-2 cells were transfected with 20 ng of reporter constructs and 1 mg of pcDNA3.1-Twist in combination with 0.2 ng of pRL-TK vector for 24 h under normoxia or low oxygen. The luciferase results are reported as relative light units of firefly luciferase activity normalized with respect to the *Renilla* luciferase activity. Mean values from three independent experiments. $^{\#}p < 0.05$ and $^{*}p < 0.01$ compared with control. (D) qChIP assay of the Bmi1 promoter region in HK-2 cells transfected with empty pcDNA3.1 vector, overexpressing Twist under normoxia or low oxygen. Increased Twist-binding levels were found in HK-2 cells under normoxia and transfected with Twist compared with control cells. In addition, compared with cells under normoxic conditions, an additional increase in Twist-binding levels was noted in hypoxic cells transfected with Twist. Data represent means ± SD ($n = 3$). The antibodies used in qChIP are indicated at the top; IgG was used as a control.

We further investigated whether Bmi1 was a target of HIF-1a. By in silico analysis, we found four sites sharing homology with the HIF-1a–binding consensus sequence BDCGTV (B = C/T/G, D = A/G/T, V = G/C/A; Sun *et al.*, 2009). To identify the transcriptional regulation of Bmi1 by HIF-1a, we constructed luciferase reporter constructs containing various lengths of Bmi1 promoter or mutated HRE (Figure 2B) and tested the effects of HIF-1a on their activity. As shown in Figure 2B, HK-2 cells were transiently cotransfected with the Bmi1 wild-type promoter vector (from –502 to +148 base pairs) or mutation vectors or pGL-basic control vector and HIF-1a. The luciferase activity increased by (5.45 ± 0.98)-fold in cells transfected with the Bmi1 wild-type promoter vector compared with that of mutation vectors ($p < 0.01$). However, the reporters containing the HRE1 mutation and/or HRE2 mutation and/or HRE3 mutation region of Bmi1 promoter showed no different luciferase activity compared with pGL-Bmi1 (wild type) vector–transfected cells. These findings suggest that hypoxia-induced expression of Bmi1 was transcriptionally dependent on HIF-1a and that the HRE4 region of Bmi1 should be the major target-binding site for HIF-1a.

Next we performed a chromatin immunoprecipitation (ChIP) assay to examine whether HIF-1a associates with the HRE sites in the Bmi1 promoter. As shown in Figure 2C, ChIP analysis of nuclei derived from HK-2 cells revealed a dominant band of 204 base pairs containing the fourth possible binding site (–190 to –185) in the hypoxic condition. No bands were evident in the other three possible binding sites and the control immunoglobulin G (IgG) immunoprecipitates. These results suggest that the proximal HRE4 at –190 was the main HIF-1a–binding site in the Bmi1 promoter.

Cooperative activation of Bmi1 by HIF-1α and Twist

Our previous work demonstrated that HIF-1α could transactivate the expression of Twist under hypoxia, and Twist was reported to bind to the promoter of Bmi1 and transcriptionally activate Bmi1 expression (Sun *et al.*, 2009; Yang *et al.*, 2010). On the basis of this and the results described here earlier, we hypothesized that HIF-1α might promote the expression of Bmi1 by directly binding to its promoter or indirectly via Twist under hypoxic conditions. We further investigated the correlation of HIF-1α and Twist simultaneously binding to and activating the Bmi1 promoter. As shown in Figure 3, qRT-PCR and Western blot assay showed that hypoxia and Twist transfections both induced Bmi1 mRNA and protein expression. Transfection with Twist under low oxygen in HK-2 cells showed higher Bmi1 mRNA and protein than treatment with Twist or hypoxia alone (Figure 3A). siRNA against Twist or HIF-1α transfection effectively reversed hypoxia-induced Bmi1 protein expression (Figure 3B).

We then performed a promoter-activity assay to investigate whether Bmi1 promoter activation is induced cooperatively by HIF-1α and Twist. Hypoxia or Twist transfection induced (6.85 ± 0.71)- or (4.31 ± 0.32)-fold Bmi1-luc900 promoter activity compared with control HK-2 cells, respectively. The wild-type Bmi1-luc900 promoter contains both a Twist-binding region at –732 to –727 and an

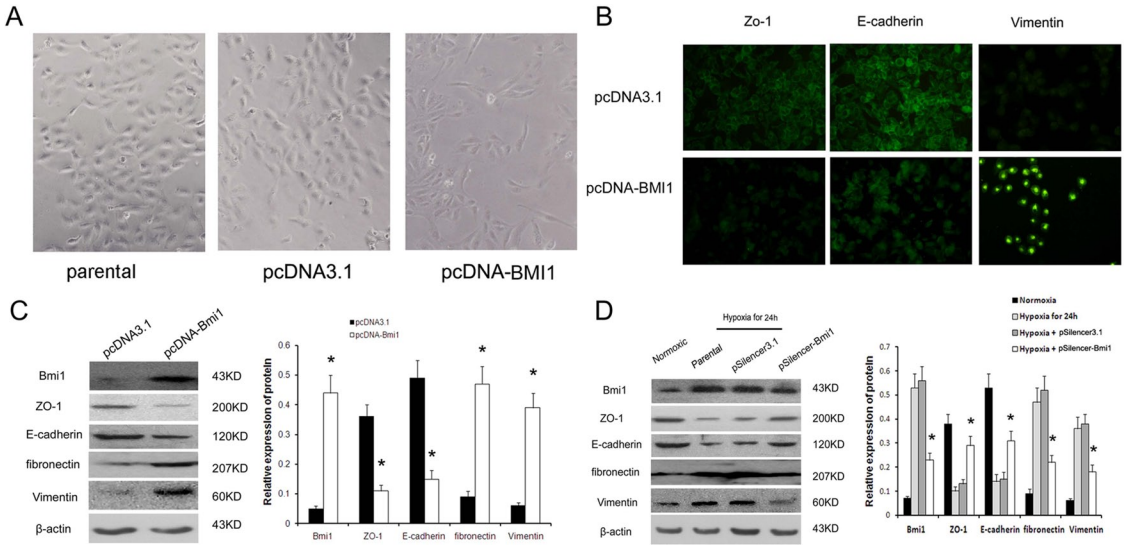

FIGURE 4: Bmi1 induces EMT in HK2 cells under hypoxic conditions. (A) Morphological changes in cells. Both parental and pcDNA3.1-transfected cells showed a typical cuboidal epithelial shape, whereas Bmi1-transfected cells were elongated and larger than control cells, consistent with the morphology of myofibroblasts. Magnification, 200×. (B) Immunofluorescence analysis of ZO-1, E-cadherin, and vimentin expression in Bmi1 and control vector–transfected HK-2 cells. (C) Western blot analysis of ZO-1, E-cadherin, fibronectin, and vimentin expression in Bmi1 and control vector–transfected HK-2 cells. Left, representative blot from three independent experiments. Right, histogram showing the average volume density normalized to the loading control, β-actin. (D) Western blot analysis of Bmi1, ZO-1, E-cadherin, fibronectin, and vimentin expression in parental cells, pSilencer3.1 empty vector–transfected cells, and Bmi1 siRNA–transfected cells after 24 h under hypoxic conditions. *$p < 0.01$ compared with parental cells and pSilencer empty vector cells.

HIF-1α–binding region at −190 to −185. Moreover, transfection with Twist under low oxygen in HK-2 cells showed higher Bmi1-luc900 promoter activity than transfection with Twist ([2.62 ± 0.21]-fold) or hypoxia ([1.68 ± 0.18]-fold) alone. Twist transfection did not increase Bmi1-luc900Mut1 promoter activity, whereas hypoxia could facilitate this reporter activity, which could not be inhibited by siRNA against Twist, suggesting that hypoxia might induce Bmi1 activation in a Twist-independent manner. It is interesting that hypoxia or Twist transfection induced Bmi1-luc900Mut2 promoter activity in which the HIF-1α–binding site (HBS) was mutated and which could be abolished by Twist siRNA transfection, suggesting that hypoxia might induce Bmi1 activation in a Twist-dependent manner. Hypoxia and/or Twist transfection did not induce Bmi1-luc900Mut3 promoter activity in which both the Twist-binding site and HBS were mutated. Quantitative ChIP (qChIP) confirmed the direct binding of Twist to the Bmi1 regulatory region. Increased Twist-binding levels were found in HK-2 cells under normoxic conditions for transfection with Twist compared with control cells. Compared with cells under normoxic conditions, additional increase in Twist-binding levels was noted in hypoxic cells transfected with Twist (Figure 3D). These results demonstrated that Twist directly activates Bmi1 transcription by binding to the promoter of the Bmi1 gene. Taking the results together, it seems that hypoxia might promote the activation and expression of Bmi1 both in HIF-1α– and in HIF-1α-Twist–mediated manners in HK-2 cells.

Bmi1-mediated, hypoxia-induced EMT in tubular epithelial cells

To investigate the functionality of Bmi1 induction, we examined the effect of overexpression of exogenous Bmi1 on tubular epithelial cell phenotypes. We established stable cell lines that overexpress Bmi1 by transfecting with either the expression vector of the Bmi1 or empty vector. As shown in Figure 4A, light microscopy revealed that parental cells and empty vector–transfected cells formed a cobblestone-like monolayer, which is typical of epithelia. Bmi1-transfected cells also formed an epithelial monolayer, but there were larger gaps between cells, and the cells were larger and more elongated than control cells. Figure 4B shows the immunofluorescence staining of E-cadherin, zonula occludens-1 (ZO-1), and vimentin in tubular epithelial cells. Compared with the empty vector controls, overexpression of Bmi1 resulted in disappearance of E-cadherin and ZO-1 staining in plasma membrane, whereas vimentin expression dramatically increased in cytoplasm. Western blots were performed to confirm that the EMT phenotype is induced in renal tubular cells by Bmi1. Expression of exogenous Bmi1 induced fibronectin and vimentin expression, whereas E-cadherin and ZO-1 expression was markedly reduced in Bmi1-overexpressing cells (Figure 4C). Hence it seems that Bmi1 triggers E-cadherin and ZO-1 suppression and vimentin and fibronectin induction, the reciprocal changes associated with the phenotypic transition from epithelial to mesenchymal.

Next we ask whether Bmi1 is involved in hypoxia-induced HK-2 cell EMT. siRNA against Bmi1 and scramble siRNA were transfected into HK-2 after 24 h under low oxygen. After another 48 h, the cells were collected, and the expression of E-cadherin, ZO-1, fibronectin, and vimentin was detected by Western blot. After 24 h of hypoxia, the levels of E-cadherin and ZO-1 protein were significantly reduced compared with levels in normoxic cells, whereas the protein fibronectin and vimentin were up-regulated in hypoxic cells (Figure 4D). These changes are all characteristic of myofibroblasts. Transfection with siRNA against Bmi1 reversed the decrease in E-cadherin and ZO-1 to the level present in normoxic cells (Figure 4D). Expression of fibronectin and vimentin were correspondingly reduced in hypoxic cells after transfection with Bmi1 siRNA (Figure 4D). In summary, Bmi1 mediated hypoxia-induced EMT in tubular epithelial cells.

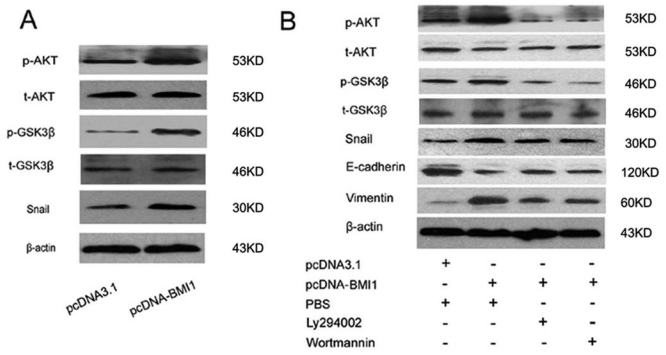

FIGURE 5: Bmi1 Activates PIK/AKT and stabilization of Snail. (A) Western blot analysis of Akt, GSK-3β, Snail, phosphorylated-Akt, and phosphorylated-GSK-3β in Hk2 cells under normoxia. (B) Western blot analysis of Akt, GSK-3β, Snail, E-cadherin, vimentin, p-Akt, and p-GSK-3β expression in Ly294002- or wortmannin-treated HK-2 cells under normoxia. Representative blot from three independent experiments.

Bmi1 activates PI3K/AKT signal in HK-2 cells

Because up-regulation of Bmi1 activates the PI3K/Akt/GSK-3β pathway, and stabilization of Snail in tumor cells and activation of the PI3K/Akt pathway are emerging as central features of renal tubular cell EMT (Zeng *et al.*, 2008; Song *et al.*, 2009; Guo *et al.*, 2011), we asked whether Bmi-1 regulates Akt activity and stabilization of Snail in HK-2 cells. As shown in Figure 5A, up-regulation of Bmi1 did not increase the total amount of Akt in HK-2 cells, whereas Akt phosphorylation was induced in cells transduced with Bmi-1. The increase in Akt phosphorylation was accompanied by a change in phosphorylation of GSK-3β and up-regulation of Snail, a downstream target protein of Akt, suggesting that up-regulation of Bmi1 activates the Akt/GSK-3β/Snail pathway in HK-2 cells.

In addition, the PI3K inhibitors wortmannin and LY29004 were used to investigate whether the stabilization of Snail and induction of EMT were caused by activation of the PI3K/Akt/GSK-3β pathway. As shown in Figure 5B, treatment with wortmannin or Ly29004 partially reversed the increase in E-cadherin to the level present in control cells. Expression of vimentin was correspondingly reduced in Bmi1-transfected cells after treatment with wortmannin or Ly294002. In addition, the expression of phosphorylated Akt was reduced by wortmannin or Ly29004 treatment, leading to further reduction of Snail. These results demonstrated that up-regulation of Bmi1 induce tubular epithelial EMT at least partly by activation of the PI3K/Akt/GSK-3β pathway and stabilization of Snail.

Bmi1 participates in hypoxia-induced renal fibrosis

To investigate the relevance of Bmi1 induction to renal fibrosis in vivo, we examined the expression of Bmi1 in the evolution of renal interstitial fibrosis induced by ureteral obstruction. Immunohistochemical staining showed that the staining of E-cadherin was decreased and that vimentin staining was increased in the kidneys of these animals in a time-dependent manner, suggesting the renal tubular epithelial cells were undergoing EMT (Supplemental Figure S2). As shown in Figure 6A, Bmi1, predominantly located in the nuclei of renal tubular epithelial cells, was markedly induced in the fibrotic kidney in at time-dependent manner, which was consistent with HIF-1α and Twist expression. Western blot analyses revealed that Bmi1 protein began to increase as early as day 1 after unilateral ureteral obstruction (UUO), and significant induction was observed at 3 d (Figure 6B), at time preceding the onset of EMT in this model (Yang *et al.*, 2002). Semiquantitative determinations showed ~18-fold induction of the relative abundance of Bmi1 protein in the obstructed kidney at 7 d after ligation compared with day 1 after ligation. Hence HIF-1α/Twist-Bmi1 induction correlates with tubular EMT and renal interstitial fibrogenesis in vivo.

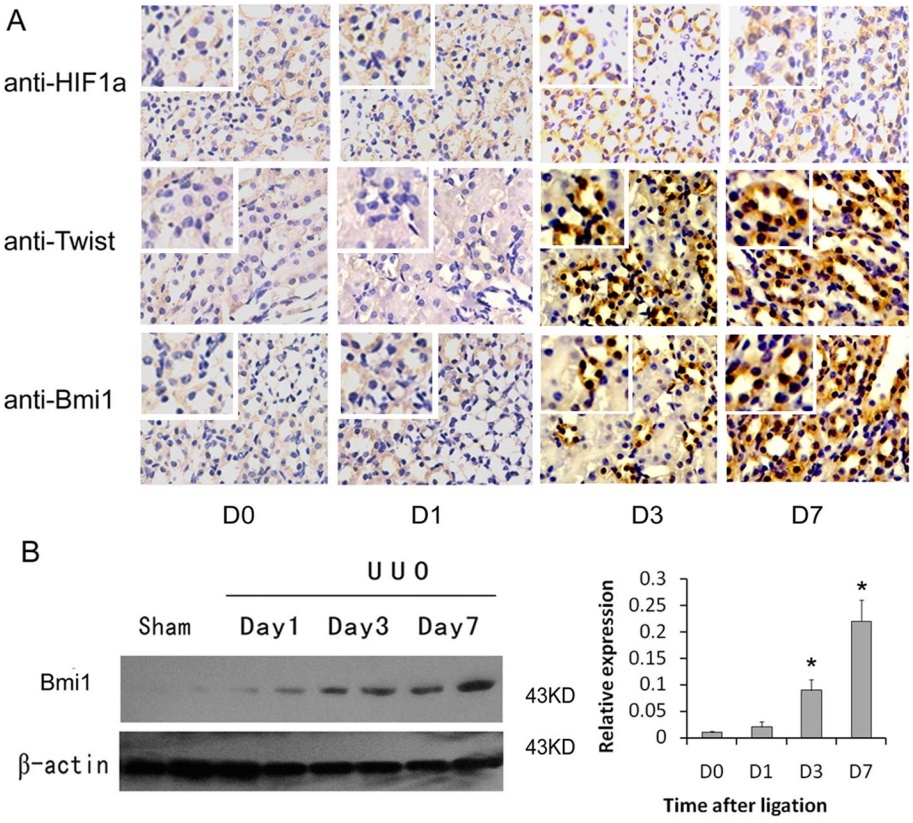

FIGURE 6: Bmi1 participates in hypoxia-induced renal fibrosis in vivo. (A) Immunohistochemical analysis for HIF-1α, Twist, and Bmi1 in the kidney tissue of UUO rats and sham-operated rats. Increased HIF-1α, Twist, and Bmi1 staining was observed in tissues of UUO rats. Original magnification, 200×. Top left insets, higher-magnification images (400×). (B) Western blot analyses indicating the induction of Bmi1 protein in fibrotic kidney. Samples from two representative animals were used at each time point. Left, representative blot from three independent experiments. Right, histogram showing the average volume density normalized to the loading control, β-actin ($n = 3$). *$p < 0.01$ compared with sham control.

Bmi1 is overexpressed in renal tissue samples from chronic kidney disease patients and associated with HIF-1a and Twist expression

After demonstrating that Bmi1 is activated in a mouse model of renal fibrosis, we next examined the extent of Bmi1 in a series of archival renal biopsy tissues from IgA nephropathy (IgAN) and diabetic nephropathy (DN) patients who had tubulointerstitial injury and chronic hypoxia (Nangaku, 2006).

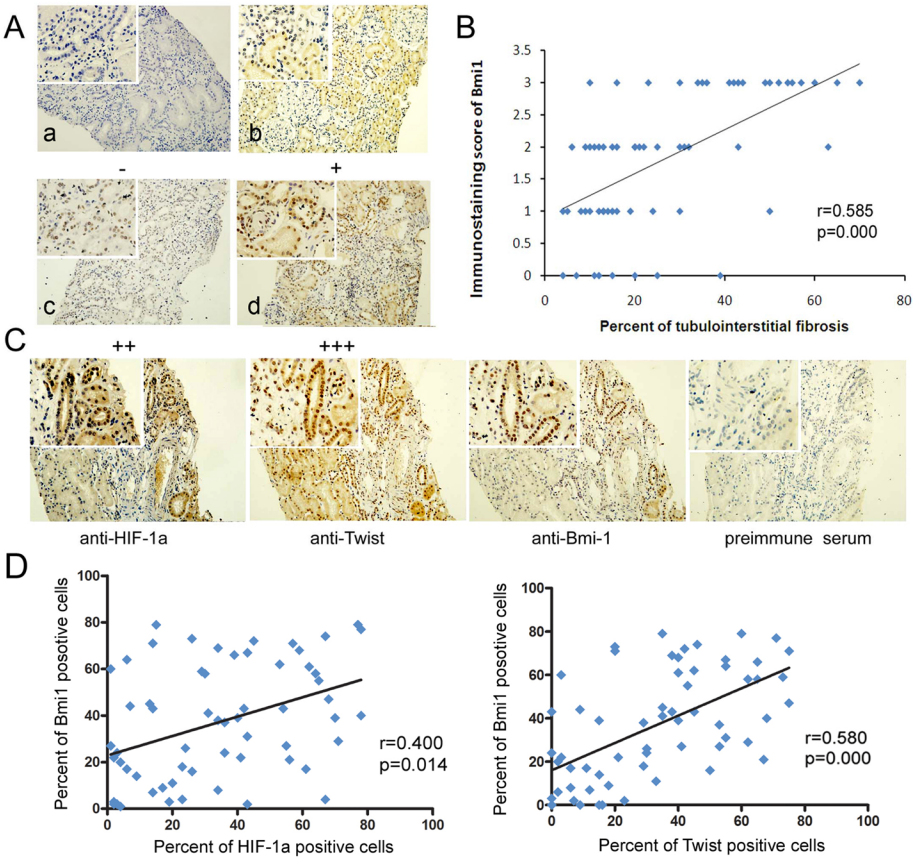

FIGURE 7: Coexpression of HIF-1α, Twist, and Bmi1 in renal biopsies from patients with CKD. (A) Bmi1 immunostaining in renal biopsy tissues from patients with IgAN (original magnification, 200×). (a) Negative control. (b) Tissue from IgAN kidney, with 1+ staining (≤25% cells positive/visual field). (c) Representative photographs from IgAN kidneys with 2+ staining (25–50% cells stained positive/visual field). (d) Representative photographs from IgAN kidneys with 3+ staining (>50% cells stained positive/visual field). Arrows highlight cells with nuclear Bmi1 staining. Top left insets, higher-magnification images. (B) Scatter plot with fitted values intervals for tubular expression of Bmi1 and tubulointerstitial fibrosis. (C) Representative pictures of the immunohistochemistry analyses of HIF-1α, Twist, and Bmi1 in consecutive sections of renal tissues from patients with IgAN (original magnification, 200×). Top left insets, higher-magnification images. (D) Scatter plot with fitted values intervals (percentage of positive cells) for tubular expression of Bmi1 and HIF-1α (left) and Bmi1 and Twist (right).

Paraffin-embedded renal tissues from 43 patients with IgAN, 18 patients with DN, and eight normal kidneys (living donor biopsies) were examined for Bmi1 expression. Tissue sections were analyzed for cellular sublocalization of staining and scored based on the percentage of Bmi1-expressing cells. As shown in Figure 7A, Bmi1 was predominantly located in the nuclear region of renal tubular epithelial cells from IgAN patients. Whereas little positive staining for Bmi1 was found in the renal tubules of normal kidneys (Bmi1 score of ≤1 and absent in glomeruli; Figure 7A), prominent Bmi1 staining (>25% of all cells positive) was found in 26 of 43 patients with IgAN and 12 of 18 patients with DN ($p = 0.018$ and 0.021, respectively, compared with normal controls, when grouped by score of ≥2+ or <2+; Fisher's exact tests; Supplemental Table S1).

To clarify the potential role or involvement of Bmi1 in the progression of chronic kidney disease (CKD), we examined the correlation between the percentage of tubulointerstitial fibrosis and staining of Bmi1. The expression of Bmi1 proteins in the tubulointerstitium was positively correlated with the percentage of tubulointerstitial fibrosis ($r = 0.585$, $p = 0.000$; Figure 7B). These results indicate that the expression of active Bmi1 correlates with the degree of tubulointerstitial fibrosis in CKD patients. Furthermore, we analyzed whether the expression of Bmi1 correlated with HIF-1α and Twist. The present work demonstrated that positive HIF-1α and Twist were observed in the nuclei in 59.0% (36/61) and 65.6% (40/61) of CKD kidney tissues, respectively (Figure 7C and Supplemental Table S2). The percentage of Bmi1-positive cells in the tubulointerstitium was closely associated with those of HIF-1α and Twist ($r = 0.400$ and $p = 0.014$, and $r = 0.580$ and $p = 0.000$, respectively; Figure 7D). These results confirm our previous finding that HIF-1α and Twist can regulate Bmi1 expression in vitro and in vivo.

DISCUSSION

The results presented in this study demonstrate that Bmi1, a member of the PcG family of transcription repressors, plays a critical role in mediating EMT in tubular epithelial cells induced by hypoxia. We showed that Bmi1 expression is induced during hypoxia-mediated EMT, and such induction is dependent on, at least in part, HIF-1α/Twist signaling, a signal pathway that is essential for EMT (Keith and Simon, 2007; Yang *et al.*, 2008). Moreover, Bmi1 induces the stabilization of Snail via modulation of PI3K/Akt signaling, and blockage of PI3K/Akt results in complete blockade of Bmi1-mediated Snail induction. Finally, Bmi1 is up-regulated in the obstructed kidney, and its expression is associated with renal interstitial fibrosis in vivo. These observations, together with previous studies (Sun *et al.* 2009, 2012b), established that HIF-1α/Twist-Bmi1 may act as a functional element that plays a crucial role in mediating hypoxia-triggered EMT in tubular epithelial cells, having significant implications for the pathogenesis of renal interstitial fibrosis.

Bmi1 is a crucial molecule for EMT in many tumor cells and Madin–Darby canine kidney cells (Song *et al.*, 2009; Wellner *et al.*, 2009; Yang *et al.*, 2010; Dong *et al.*, 2011; Sun *et al.*, 2012a); however, little is known about its regulation and function in renal fibrosis. This study provides evidence that Bmi1is involved in hypoxia-induced EMT in renal tubular epithelial cells and renal fibrosis. Enforced expression of exogenous Bmi1 leads to loss of E-cadherin and ZO-1 and induction of fibronectin in HK-2 cells. Conversely, knockdown of Bmi1 completely blocks hypoxia-mediated fibronectin expression and partially restores E-cadherin, suggesting a functional role of Bmi1 in hypoxia-induced EMT in renal tubular epithelial cells in vitro. The UUO fibrosis model was initially established to study TGF-β–induced renal fibrosis. Research by Higgins' team identified this as a chronic hypoxia renal fibrosis model (Higgins *et al.* 2007). Immunochemistry results showed that HIF-1α protein was increased expression in renal epithelial cells on days 3 and 7 after ligation, which was consistent with previous work. In addition, Twist and Bmi1 protein were up-regulated in renal epithelial cells on days 3 and 7 after ligation. Indeed, Western blot analysis showed a marked induction of Bmi1 in the fibrotic kidney induced by UUO in

a time-dependent manner. Moreover, we found that Bmi1 expression was increased in the tubulointerstitial compartment of kidneys from patients with IgA and diabetic nephropathy; the distribution pattern of Bmi1 is highly congruent with the percentage of tubulointerstitial fibrosis, supporting the notion that Bmi1 may play a role in the development and progression of renal fibrosis. In conclusion, our experimental data provide clear in vitro and in vivo evidence for the first time that Bmi1 is involved in hypoxia-induced EMT in human renal tubular epithelial cells and renal fibrosis.

Chronic hypoxia and tubulointerstitial injury are final common pathways in progression to end-stage renal disease (Nangaku, 2006). Research by Higgins' team showed that HIF-1α– induced EMT in tubular epithelial cells plays an essential role in renal fibrosis under chronic low oxygen (Higgins *et al.*, 2007). HIF-1α could bind to the promoter of a wide range of target genes by the hypoxia-responsive element and certain transactivated EMT regulators, such as Snail, Zeb1, SIP1, E47/TCF3, CTGF, and lysyl oxidase (Imai *et al.*, 2003; Erler *et al.*, 2006; Krishnamachary *et al.*, 2006; Evans *et al.*, 2007). Here we demonstrate that direct regulation of Twist, a master regulator of mesoderm development (Yang *et al.*, 2004), by HIF-1α promotes EMT in renal tubular epithelial cells and fibrosis. However, the molecular mechanisms of hypoxia-induced EMT in kidney tubular epithelial cells are complicated, and Twist downstream signal pathways are far from elucidated. Bmi1 was identified as a Twist-responsive transcription factor and could be induced by hypoxia in tumor cells (Yang *et al.*, 2010). In the present study, our experimental data demonstrate that Bmi1 transcriptional activation is cooperatively induced by HIF-1a and Twist. This is based on the following observations. First, the mRNA and protein levels of Bmi1 were up-regulated in HK-2 cells after induction of hypoxia or transfection with Twist, and transfection with Twist under hypoxia induced much higher mRNA and protein levels of Bmi1 than did induction of hypoxia or transfection with Twist alone in HK-2 cells, whereas siRNA against HIF-1a or Twist abolished hypoxia-induced Bmi1 expression and nuclei accumulation. Second, bioinformatic analysis showed that the region of Bmi1 promoter contains four hypoxia-responsive region sites and one E-box (Twist-binding) region site. The roles of HREs and Twist-responsive elements of the promoter Bmi1 were clarified by a luciferase reporter system. According to Figure 3, hypoxia or transfection with Twist augmented Bmi1 promoter luciferase activity. Compared with cells under normoxic conditions, additional threefold increase in relative luciferase activity was noted in hypoxic cells transfected with Twist. ChIP assay confirmed HRE4 in the Bmi1 promoter as a direct HIF-1a–binding site. Third, in vivo, we showed that Bmi1 occurred in fibrotic kidney tissue from patients with CKD and the UUO fibrosis rat model and was mainly located in nuclei of renal tubule cells. In addition, the distribution pattern of Bmi1 is highly congruent with that of HIF-1a and Twist in both fibrotic kidney tissues from patients with CKD and the UUO fibrosis rat model. These results indicate that HIF-1a and Twist cooperatively promoted Bmi1 transcriptional activation under low oxygen. The results from these studies specified the sequence −190 to −185 as a classic HRE, and the mutation of this HBS results in a complete blockage of HIF-1a–binding activity. To our knowledge, our data show for the first time that HIF-1a can directly transactivate the Bmi1 promoter by binding to the sequence −190 to −185 of the Bmi1 promoter in response to hypoxia. Previous work showed that hypoxia could induce Bmi1 expression and transcriptional activation via activation of Twist in tumor cells (Yang *et al.*, 2010).

Bmi1 is a member of the PcG gene group, which is a group of transcriptional repressors that play essential roles in the maintenance of appropriate gene expression during development (Lund and van Lohuizen, 2004; Boyer *et al.*, 2006; Bracken *et al.*, 2006; Lee *et al.*, 2006; Schwartz *et al.*, 2006). Accumulating evidence suggests that Bmi1 is expressed in a variety of tumor populations and promotes tumor metastasis by modulating the EMT process (Song *et al.*, 2009; Yang *et al.*, 2010, 2012). The downstream signal pathway for Bmi1-induced EMT has been well established. Song *et al.* (2009) demonstrated that Bmi1 transcriptionally down-regulated expression of the tumor suppressor PTEN in tumor cells by direct association with the PTEN locus, which in turn led to dysfunction of PI3K/Akt/GSK-3β signaling and the stabilization of Snail. Wang's group reported that Bmi1 and Twist act cooperatively to repress E-cadherin in head and neck squamous cell carcinoma (Yang *et al.*, 2010). This group recently showed that Twist cooperates with Bmi1 to suppress let-7i expression, which results in up-regulation of NEDD9 and DOCK3, leading to RAC1-activated EMT phenotype in three-dimensional environments (Yang *et al.*, 2012). In the present study, we focused on the relationship between Bmi1 and activation of the PI3K/Akt pathway because the PI3K/Akt pathway is well known for its central role in hypoxia-induced EMT in renal tubular epithelial cells and renal fibrosis (Rodríguez-Peña *et al.*, 2008; Zeng *et al.*, 2008). We observed activation of PI3K/Akt in Bmi1-induced EMT, which correlates with hyperphosphorylated GSK-3β, Snail stabilization, and E-cadherin down-regulation. The transcriptional activity of Snail is regulated by GSK-3β, which is negatively regulated by PI3K/Akt (Zhou *et al.*, 2004; Bachelder *et al.* 2005). Treatment with Ly294002 or wortmannin abolished the Bmi1-induced EMT phenotype, accompanied by restoration of E-cadherin and decreased vimentin. At the same time, phosphorylation of Akt was decreased and induction in Snail was reduced. Therefore, our experimental data demonstrate that the PI3K/Akt pathway might play a critical role in Bmi1-induced EMT.

In conclusion, our findings provide mechanistic insight into hypoxia induction of EMT and renal fibrosis via up-regulation of Bmi1. Uncovering a novel function and molecular mechanism for Bmi1 overexpression in hypoxia-induced EMT provides important insight into understanding renal fibrosis and antifibrogenesis strategies.

MATERIALS AND METHODS

Cell culture

Human proximal tubular epithelial cell lines (HK-2) were used as described earlier (Sun *et al.*, 2009). HK-2 cells were cultured in DMEM/F12 (Invitrogen, Carlsbad, CA), supplemented with 10% fetal calf serum. HKC cells were cultured in DMEM (GIBCO, Grand Island, NY) supplemented with 10% fetal calf serum. (Life Technologies-BRL Life Technologies, Burlington, Canada). For hypoxic culture, cells were placed in a hypoxic (1% O_2, 5% CO_2, 37°C) incubator (Precision Scientific, Winchester, VA) for 0, 2, 6, 12, 24, 48, or 72 h. Control cells (normoxic cells) were incubated for equivalent periods under normoxic conditions (21% O_2, 5% CO_2, 37°C).

Quantitative RT-PCR

Total RNA was extracted from cells (2×10^6) and rat renal tissues (0.1 mg) using TRIzol (Invitrogen) according to the manufacturer's protocol. Aliquots (5 mg) of RNA were reverse transcribed to cDNA using the Superscribe First-Strand Synthesis System (Invitrogen). Specific primers were designed; the primers and amplicons are given in Supplemental Table S3. qRT-PCR was conducted according to the manufacturer's instructions (Invitrogen). Reactions were run on a real-time PCR system (ABI PRISMH 7700; Applied Biosystems, Foster, CA). Gene expression was detected with the SYBR Green RT-PCR Kit (Invitrogen), and relative gene expression was

determined by normalizing to glyceraldehyde-3-phosphate dehydrogenase using the $2^{-\Delta\Delta CT}$ method (Du *et al.*, 2012).

Protein preparation and Western blot

Fresh tissue blocks (0.1 mg) or harvested cells (2×10^6) were put into 1.5-ml Eppendorf tubes and homogenized with 400 µl of lysis buffer (50 mmol/l Tris-HCl, pH 8.0, 150 mmol/l NaCl, 0.1% SDS, 1% Nonidet P-40, 0.5% sodium deoxycholate, 0.02% sodium azide, 100 µg/ml phenylmethylsulfonyl fluoride, 1 µg/ml aprotinin). The tissue samples were then homogenized by ultrasonic vibration and heated at 95°C for 5 min. Cell lysates were centrifuged at 4°C for 5 min at 10,000 rpm, and the protein-containing supernatant was removed to fresh tubes for experimental purposes. Protein concentration was measured using the Bio-Rad (Hercules, CA) protein assay kit.

For Western blot, total protein (60 µg) was electrophoresed on 10% SDS–polyacrylamide gels and then transferred to nitrocellulose membranes (Millipore, Bedford, MA). After blocking with 10% fat-free milk in Tris-buffered saline (20 mmol/l Tris, 0.15 mol/l NaCl, pH 7.0, 0.1% Tween 20), the membranes were incubated with a primary antibody: HIF-1a (1:1000; Chemicon, Bedford, MA), Twist antibody (1:200; Santa Cruz Biotechnology, Santa Cruz, CA), Bmi1 antibody (1:1000; Sigma-Aldrich, St. Louis, MO), E-cadherin (1:200; Santa Cruz Biotechnology), ZO-1 (1:400; Chemicon), fibronectin (1:100; Santa Cruz Biotechnology), vimentin (1:200; Santa Cruz Biotechnology), Snail (1:100; Santa Cruz Biotechnology), and Akt, p-Akt, GSK-3β, and p-GSK-3β (1:1000, Cell Signaling Technology, Danvers, MA). After repeated washing, the membranes were incubated with horseradish peroxidase–conjugated anti-rabbit or anti-mouse secondary antibody (Santa Cruz Biotechnology) diluted 1:2000. The bands were visualized using the enhanced chemiluminescence system (Amersham Pharmacia Biotech) and exposed to Kodak X-OMAT film (Rochester, NY). Western blot for β-actin was performed as an internal sample loading by using mouse monoclonal antibody (1:5000; Sigma-Aldrich).

Plasmid constructs and cell transfection

The recombinant sense expression vectors for HIF-1a, Twist, and the siRNA expression vectors against HIF-1a and Twist were constructed as described earlier (Sun *et al.*, 2009). Human Bmi-1 was amplified by PCR using cDNA from hypoxia-induced human renal tubular epithelial cells (HK-2) and subcloned into pCDNA3.1 expression vector. Target siRNA was determined using the siRNA design tool (Invitrogen). The Bmi1 siRNA–specific targeting sequence was 5'- GACCAGACCACTA-CTGAAT-3'; a scramble sequence was used as control. The sequences were checked against the database to confirm specificity and were cloned into the pSilencer3.1-U6 neo siRNA expression vector (Ambion, Austin, TX).

For luciferase reporter experiments, Bmi1 promoter–driven luciferase reporter vector Bmi1-Luc900, which contains one putative Twist-binding site and four HBSs, was constructed by inserting the wide-type sequence (from –877 to +23 base pairs) of the Bmi1 promoter into a pGL3-basic vector. Bmi1-Luc900Mut1, Bmi1-Luc900Mut2, and Bmi1-Luc900Mut3 were constructs with mutations in the Twist-binding site and/or HBS in Bmi1-Luc900. To assay the transcriptional activity of Bmi1 under hypoxic condition, a set of Bmi1 promoter-driven luciferase reporter vectors was constructed by inserting the wild-type sequence (from –477 to +23 base pairs), one truncated sequence (from –242 to +23 base pairs), HRE1 mutants (GACGTA mutated to GAAATA), and/or HRE2 mutants (GGCGTG mutated to GGAAGG), and/or HRE3 (CGCGTG mutated to CGAAGG), and/or HRE4 (CACGTG mutated to CAAAGG) of the Bmi1 promoter into a pGL3-basic vector (Promega, Madison, WI), respectively.

Bioinformatic analysis of HIF-1– and Twist-binding sites

A genomic region of 1200 base pairs upstream of the Bmi1 transcriptional initiation site was determined using the National Center for Biotechnology Information Genomic BLAST program. This DNA sequence was then pasted into DNA Strider 1.0 software, which was used to locate putative Twist1-binding sites and HBSs. The search was based on compilations of functional HBSs and the HIF-1–binding consensus sequence BDCGTV (B = C/T/G; D = A/G/T; V = G/C/A; Sun *et al.* 2009), in turn established by following definitions of consensus sequences.

Dual-luciferase reporter gene assay

HK-2 cells in a 24-well plate (20,000 cells/well) were cotransfected with pcDNA-HIF-1α (200 ng) and/or pcDNA-Twist (200 ng) and the reporter plasmid using Lipofectamine 2000 (Invitrogen), with 80 ng of PRL-TK (Promega) as a control for transfection efficiency in DMEM without serum. Luciferase activity was measured 48 h after transfection using the Dual Luciferase Reporter Assay System (Promega). Firefly luciferase activity was normalized to *Renilla* luciferase activity for each transfected well. Three independent experiments were performed in triplicate.

ChIP assay and qChIP

HIF-1α and Twist binding to Bmi1 promoter was analyzed by ChIP on HK-2 cells, using methodologies described earlier (Sun *et al.*, 2009). HK-2 cells were fixed with 1% paraformaldehyde, and chromatin derived from isolated nuclei was sheared by using an F550 microtip cell sonicator (Fisher Scientific, Waltham, MA). After centrifugation, supernatants containing sheared chromatin were incubated with an anti–HIF-1α/Twist antibody or control IgG. Protein A–Sepharose was then added before the overnight incubation, and the immune complexes were subsequently eluted. Complexes were next treated with RNase and proteinase K and were extracted with phenol/chloroform and then with chloroform. DNA was precipitated, washed, dried, resuspended in water, and analyzed by PCR or qPCR. The primers and amplicons of PCR in this analysis are listed in Supplemental Table S3.

Immunofluorescence staining and immunocytochemistry

Indirect immunofluorescence staining was performed using an established procedure (Sun *et al.*, 2009). Briefly, cells cultured on coverslips were washed with cold phosphate-buffered saline (PBS) twice and fixed with cold methanol:acetone (1:1) for 10 min at –20°C. After extensive washing three times with PBS containing 0.5% bovine serum albumin, the cells were blocked with 20% normal donkey serum in PBS buffer for 30 min at room temperature and then incubated with the specific primary antibodies against E-cadherin, ZO-1, α-SMA, and vimentin as described previously. For visualization of the primary antibodies, cells were stained with fluorescein isothiocyanate–conjugated secondary antibodies (Jackson ImmunoResearch Laboratories, West Grove, PA). As a negative control, the primary antibody was replaced with nonimmune IgG, and no staining occurred. Stained cells were mounted with Vectashield mounting medium (Vector Laboratories, Burlingame, CA) and viewed with an Eclipse E600 epifluorescence microscope equipped with a digital camera (Nikon, Melville, NY).

Immunohistochemstry was carried out as described earlier using the Avidin–Biotin Complex (ABC) Vectastain Kit (Vector

Laboratories) according to the manufacturer's instructions. Briefly, 3- to 5-μm-thick tissue slides were dewaxed, rehydrated, incubated with 3% hydrogen peroxide for 30 min, and blocked in 10% normal goat or rabbit serum for 1 h. The slides were then incubated with primary antibodies, including HIF-1α (1:500; Chemicon), Twist antibody (1:200; Santa Cruz Biotechnology), E-cadherin (1:100; Santa Cruz Biotechnology), and Bmi1 (1:100; Sigma-Aldrich), at 41°C overnight. The sections were incubated with biotinylated goat anti-rabbit or anti-mouse Ig antibody as the secondary antibody, and the antibody reactions were visualized using diaminobenzidine (DAKO, Tokyo, Japan). Nonimmune goat IgG or rabbit IgG was used as negative control. Slides were counterstained with hematoxylin and then dehydrated and mounted. Immunostaining was evaluated in a blinded manner, as previously described (Higgins *et al*. 2007). The immunostaining score was determined by counting the HIF-1α/Twist/Bmi1–positive tubular epithelial cells under a microscope at 200× magnification on 10 random fields. A relative scale of 0–3 was used to grade the amount of HIF-1α/Twist/Bmi1 immunostaining, where 0 indicated <5% staining, 1+ indicated 5–25% staining, 2+ indicated 25–50% immunostaining, and 3+ indicated >50% immunostaining.

Animal model

Male Sprague Dawley rats (n = 24, six per group) weighing 150–180 g were obtained from the Fourth Military Medical University laboratory animal center (Xi'an, China). UUO was performed using an established procedure, as described previously. Rats were killed at various time points as indicated after surgery, and kidneys were removed. The samples were stored in −80°C until analysis. All animal handling conformed to the guidelines for care and use of experimental animals established by the Ethical Committee of Animal Experiments.

Kidney biopsies

Renal biopsy samples from patients diagnosed with CKD at Xijing Hospital from January 2010 to June 2011 were reviewed and selected for further study. Formalin-fixed and paraffin-embedded samples of IgAN (n = 43) and DN (n = 18) were identified in the Pathology Department of Xijing Hospital. Eight samples obtained from living donor biopsies were used as controls. The percentage of tubulointerstitial fibrosis was obtained from the standard pathology report (Sun *et al.*, 2012b). The study was approved by the Hospital's Protection of Human Subjects Committee, and informed consent was obtained from all patients.

Statistical analysis

Each experiment was repeated at least three times. Bands from Western blots were quantified with Quantity One software (Bio-Rad). Relative protein and mRNA levels were calculated in comparison to internal β-actin standards. Numerical data are presented as mean ± SD. The difference between means was analyzed with analysis of variance. The relationship between the scored HIF-1α or Twist expression and Bmi1 expression was assessed by a linear regression correlation test. Differences were considered significant when $p < 0.05$. All statistical analyses were done with SPSS12.0 software (SPSS, Chicago, IL).

ACKNOWLEDGMENTS

This work was partially supported by grants from the National Basic Research Program of China (973 Program; 2012CB517600, 2012CB517601) and the National Nature Science Foundation of China (81070570, 81170670, and 81270768).

REFERENCES

Bachelder RE, Yoon S-O, Franci C, de Herreros AG, Mercurio AM (2005). Glycogen synthase kinase-3 is an endogenous inhibitor of Snail transcription implications for the epithelial–mesenchymal transition. J Cell Biol 168, 29–33.

Bessede E, Staedel C, Acuna Amador LA, Nguyen PH, Chambonnier L, Hatakeyama M, Belleannee G, Megraud F, Varon C (2013). *Helicobacter pylori* generates cells with cancer stem cell properties via epithelial-mesenchymal transition-like changes. Oncogene, DOI: 10.1038/onc.2013.380.

Boyer LA, Plath K, Zeitlinger J, Brambrink T, Medeiros LA, Lee TI, Levine SS, Wernig M, Tajonar A, Ray MK, *et al.* (2006). Polycomb complexes repress developmental regulators in murine embryonic stem cells. Nature 441, 349–353.

Bracken AP, Dietrich N, Pasini D, Hansen KH, Helin K (2006). Genome-wide mapping of Polycomb target genes unravels their roles in cell fate transitions. Genes Dev 20, 1123–1136.

Dong P., Kaneuchi M, Watari H, Hamada J, Sudo S, Ju J, Sakuragi N (2011). MicroRNA-194 inhibits epithelial to mesenchymal transition of endometrial cancer cells by targeting oncogene BMI-1. Mol Cancer 10, 99.

Du R, Sun W, Xia L, Zhao A, Yu Y, Zhao L, Wang H, Huang C, Sun S (2012). Hypoxia-induced down-regulation of microRNA-34a promotes EMT by targeting the Notch signaling pathway in tubular epithelial cells. PLoS One 7, e30771.

Erler JT, Bennewith KL, Nicolau M, Dornhöfer N, Kong C, Le Q-T, Chi J-TA, Jeffrey SS, Giaccia AJ (2006). Lysyl oxidase is essential for hypoxia-induced metastasis. Nature 440, 1222–1226.

Evans AJ, Russell RC, Roche O, Burry TN, Fish JE, Chow VW, Kim WY, Saravanan A, Maynard MA, Gervais ML, *et al.* (2007). VHL promotes E2 box-dependent E-cadherin transcription by HIF-mediated regulation of SIP1 and snail. Mol Cell Biol 27, 157–169.

Guo B, Feng Y, Zhang R, Xu L-H, Li M-Z, Kung H-F, Song L-B, Zeng M-S (2011). Bmi-1 promotes the invasion and metastasis, and its elevated expression is correlated with an advanced stage of breast cancer Mol Cancer 10, 10.

Higgins DF, Kimura K, Bernhardt WM, Shrimanker N, Akai Y, Hohenstein B, Saito Y, Johnson RS, Kretzler M, Cohen CD, *et al.* (2007). Hypoxia promotes fibrogenesis in vivo via HIF-1 stimulation of epithelial-to-mesenchymal transition. J Clin Invest 117, 3810–3820.

Imai T, Horiuchi A, Wang C, Oka K, Ohira S, Nikaido T, Konishi I (2003). Hypoxia attenuates the expression of E-cadherin via up-regulation of SNAIL in ovarian carcinoma cells. Am J Pathol 163, 1437–1447.

Iwano M, Plieth D, Danoff TM, Xue C, Okada H, Neilson EG (2002). Evidence that fibroblasts derive from epithelium during tissue fibrosis. J Clin Invest 110, 341–350.

Kalluri R, Neilson EG (2003). Epithelial-mesenchymal transition and its implications for fibrosis. J Clin Invest 112, 1776–1784.

Keith B, Simon MC (2007). Hypoxia-inducible factors, stem cells, and cancer. Cell 129, 465–472.

Krishnamachary B, Zagzag D, Nagasawa H, Rainey K, Okuyama H, Baek JH, Semenza GL (2006). Hypoxia-inducible factor-1-dependent repression of E-cadherin in von Hippel-Lindau tumor suppressor-null renal cell carcinoma mediated by TCF3, ZFHX1A, and ZFHX1B. Cancer Res 66, 2725–2731.

Lee TI, Jenner RG, Boyer LA, Guenther MG, Levine SS, Kumar RM, Chevalier B, Johnstone SE, Cole MF, Isono K, *et al.* (2006). Control of developmental regulators by Polycomb in human embryonic stem cells. Cell 125, 301–313.

Liu S, Dontu G, Mantle ID, Patel S, Ahn N-S, Jackson KW, Suri P, Wicha MS (2006). Hedgehog signaling and Bmi-1 regulate self-renewal of normal and malignant human mammary stem cells. Cancer Res 66, 6063–6071.

Lund AH, van Lohuizen M (2004). Polycomb complexes and silencing mechanisms. Curr Opin Cell Biol 16, 239–246.

Mani SA, Guo W, Liao MJ, Eaton EN, Ayyanan A, Zhou AY, Brooks M, Reinhard F, Zhang CC, Shipitsin M, *et al.* (2008). The epithelial-mesenchymal transition generates cells with properties of stem cells. Cell 133, 704–715.

Nangaku M (2006). Chronic hypoxia and tubulointerstitial injury: a final common pathway to end-stage renal failure. J Am Soc Nephrol 17, 17–25.

Pirrotta V (1998). Polycombing the genome: PcG, trxG, and chromatin silencing. Cell 93, 333–336.

Rodríguez-Peña AB, Grande MT, Eleno N, Arévalo M, Guerrero C, Santos E, López-Novoa JM (2008). Activation of Erk1/2 and Akt following unilateral ureteral obstruction. Kidney Int 74, 196–209.

Schwartz YB, Kahn TG, Nix DA, Li XY, Bourgon R, Biggin M, Pirrotta V (2006). Genome-wide analysis of Polycomb targets in *Drosophila melanogaster*. Nat Genet 38, 700–705.
Song L-B, Li J, Liao W-T, Feng Y, Yu C-P, Hu L-J, Kong Q-L, Xu L-H, Zhang X, Liu W-L (2009). The polycomb group protein Bmi-1 represses the tumor suppressor PTEN and induces epithelial-mesenchymal transition in human nasopharyngeal epithelial cells. J Clin Invest 119, 3626–3636.
Sun S, Du R, Xia L, Sun W, Zhai Y, Yu Y, Zhao A, Huang C, Ning X, Wang H (2012b). Twist is a new prognostic marker for renal survival in patients with chronic kidney disease. Am J Nephrol 35, 141–151.
Sun S, Ning X, Zhang Y, Lu Y, Nie Y, Han S, Liu L, Du R, Xia L, He L, *et al*. (2009). Hypoxia-inducible factor-1alpha induces Twist expression in tubular epithelial cells subjected to hypoxia, leading to epithelial-to-mesenchymal transition. Kidney Int 75, 1278–1287.
Sun L, Yao Y, Liu B, Lin Z, Lin L, Yang M, Zhang W, Chen W, Pan C, Liu Q, *et al*. (2012a). MiR-200b and miR-15b regulate chemotherapy-induced epithelial-mesenchymal transition in human tongue cancer cells by targeting BMI1. Oncogene 31, 432–445.
Thiery JP, Acloque H, Huang RY, Nieto MA (2009). Epithelial-mesenchymal transitions in development and disease. Cell 139, 871–890.
Valk-Lingbeek ME, Bruggeman SW, van Lohuizen M (2004). Stem cells and cancer; the polycomb connection. Cell 118, 409–418.
van Lohuizen M, Verbeek S, Scheljen B, Wientjens E, van der Guidon H, Berns A (1991). Identification of cooperating oncogenes in E μ-*myc* transgenic mice by provirus tagging. Cell 65, 737–752.
Wellner U, Schubert J, Burk UC, Schmalhofer O, Zhu F, Sonntag A, Waldvogel B, Vannier C, Darling D, zur Hausen A, *et al*. (2009). The EMT-activator ZEB1 promotes tumorigenicity by repressing stemness-inhibiting microRNAs. Nat Cell Biol 11, 1487–1495.
Widschwendter M, Fiegl H, Egle D, Mueller-Holzner E, Spizzo G, Marth C, Weisenberger DJ, Campan M, Young J, Jacobs I, *et al*. (2007). Epigenetic stem cell signature in cancer. Nat Genet 39, 157–158.
Yang J, Mani SA, Donaher JL, Ramaswamy S, Itzykson RA, Come C, Savagner P, Gitelman I, Richardson A, Weinberg RA (2004). Twist, a master regulator of morphogenesis, plays an essential role in tumor metastasis. Cell 117, 927–939.
Yang J, Shultz RW, Mars WM, Wegner RE, Li Y, Dai C, Nejak K, Liu Y (2002). Disruption of tissue-type plasminogen activator gene in mice reduces renal interstitial fibrosis in obstructive nephropathy. J Clin Invest 110, 1525–1538.
Yang M-H, Hsu DS-S, Wang H-W, Wang H-J, Lan H-Y, Yang W-H, Huang C-H, Kao S-Y, Tzeng C-H, Tai S-K (2010). Bmi1 is essential in Twist1-induced epithelial-mesenchymal transition. Nat Cell Biol 12, 982–992.
Yang MH, Wu MZ, Chiou SH, Chen PM, Chang SY, Liu CJ, Teng SC, Wu KJ (2008). Direct regulation of TWIST by HIF-1alpha promotes metastasis. Nat Cell Biol 10, 295–305.
Yang WH, Lan HY, Huang CH, Tai SK, Tzeng CH, Kao SY, Wu KJ, Hung MC, Yang MH (2012). RAC1 activation mediates Twist1-induced cancer cell migration. Nat Cell Biol 14, 366–374.
Zeng R, Yao Y, Han M, Zhao X, Liu XC, Wei J, Luo Y, Zhang J, Zhou J, Wang S, *et al*. (2008). Biliverdin reductase mediates hypoxia-induced EMT via PI3-kinase and Akt. J Am Soc Nephrol 19, 380–387.
Zhou BP, Deng J, Xia W, Xu J, Li YM, Gunduz M, Hung MC (2004). Dual regulation of Snail by GSK-3beta-mediated phosphorylation in control of epithelial-mesenchymal transition. Nat Cell Biol 6, 931–940.